JSR Publications

Available Online

J. Sci. Res. **1** (2), 182-191 (2009)

JOURNAL OF SCIENTIFIC RESEARCH

www.banglajol.info/index.php/JSR

Elastic Properties of α- and β-phases of Li_3N

M. A. Hossain[1], A. K. M. A. Islam[2], and F. N. Islam[2]

[1]Mawlana Bhashani Science & Technology University, Santosh, Tangail-1902, Bangladesh

[2]Department of Physics, Rajshahi University, Rajshahi-6205, Bangladesh

Received 27 December 2008, accepted in revised form 20 March 2009

Abstract

Investigations of elastic properties of Li_3N in both α- and β-phases have been made by first-principles methods (HF-LCAO, DFT as implemented in CRYSTAL98 and in CASTEP). The theoretical equation of state of the β-phase (D^4_{6h} structure) produced by our total-energy calculations is compared with the experimental EOS. Five independent elastic constants are calculated for the first time for both the phases. These are compared with the available four elastic constants of α-Li_3N estimated from the slopes of the acoustic branches in the long wavelength region of the measured phonon dispersion curves. The aggregate elastic moduli (B, G, E), the Poisson's ratio (ν) and the Debye temperature Θ_D as a function of pressure are also calculated and the results discussed.

Keywords: Li_3N; α- and β-phases; Elastic properties; Debye temperature.

DOI: 10.3329/jsr.v1i2.1763

1. Introduction

Lithium nitride is a superionic conductor (high Li^+ conductivity of 10^3 $\Omega^{-1}cm^{-1}$ at room temperature and at zero pressure) with several interesting properties and potentials for uses [1-6]. It crystallizes in a hexagonal structure, α-Li_3N, with four ions per unit cell at ambient conditions at equilibrium pressure. This layered structure consists of Li_2N layers, widely separated by a pure Li layer which occupies a site between the nitrogen atoms in adjacent layers [1, 7]. In the Li_2N layers each N^{3+} (0, 0, 0) is at the centre of a regular hexagon formed by the six neighbouring Li^+ ions (1/3, 2/3, 0) and (2/3, 1/3, 0) in units of lattice vectors. Here N^{-3} ions, unstable as free ions, are stabilized by the electrostatic potential in the crystal environment - a hexagonal bipyramid of Li^+ ions. The unit-cell dimensions are a = 3.648 Å and c = 3.875 Å with the symmetry point group of D^1_{6h} (space group *P6/mmm*) [8].

The existence of high-pressure β- and γ-phases was confirmed in experiments and their behaviour at high pressure studied by different workers [9-13]. At ~0.5-0.6 GPa α-

[1] *Corresponding author*: anwar647@gmail.com

Li_3N was observed to transform into a layered hexagonal structure β-Li_3N ($P6_3/mmc$). Several theoretical and experimental investigations have been undertaken [14-19] to reveal the interesting properties of this superionic compound at ambient condition. All these works are followed by more recent study by Huq *et al.* [20] who investigated both α- and β-phases of commercial Li_3N using neutron powder diffraction.

The mechanical properties provide the knowledge of the practical applications of materials. Several fundamental solid-state properties, such as equation of state (EOS), specific heat, thermal expansion, Debye temperature, Grüneisen parameter, melting point and many others are closely related to elastic properties of solids, and are important in fields ranging from geophysics to materials research, chemistry and physics. The knowledge of elastic constants C_{ij} is essential for many practical applications related to the mechanical properties of materials, e.g. load deflection, sound velocities, internal strain, thermo-elastic stress. These also offer important information regarding the degree of anisotropy which is known to correlate with a tendency to either ductility or brittleness. Further solid-state variables such as electric field, magnetic field, lattice defects, phase transformation, pressure, temperature etc change the values of elastic constants. Depending on the material, the largest change usually arises from phase transformation, the smallest from electrical and magnetic fields. Further the knowledge of the values of elastic constants helps us to analyse the thermodynamic and thermo-elastic properties of ionic solids at high temperatures.

There are five independent elastic constants for hexagonal Li_3N. But no direct measurement of these is available in literature. Only four out of five C_{ij} have been determined from the slopes of the acoustic branches in the long-wavelength region obtained by the measured phonon dispersion curves [14]. The aim of the present report is to provide the *ab initio* calculations of elastic properties as well as first information on all the elastic constants of α- and β-phases of Li_3N.

2. Computational Methods

We have carried out a first-principles total-energy calculation of the structural and the elastic properties for Li_3N using two different methods. The first one is the *ab initio* CRYSTAL98 programme [21, 22] which performed Hartree-Fock, exact exchange, all electron calculations. The atomic orbitals obtained as a linear combination of *s*-, *p*-, and *d* GTO's coupled with appropriate contraction coefficients constitute the basis functions. We have followed the arguments presented by Dovesi *et al.* [17] for the use of extended and highly polarizable basis sets for the description of ionic systems. This ensures that Coulomb effects are taken into consideration accurately both in the calculation of the Fock matrix and in the evaluation of the total energy [17]. 25 *k* points in the irreducible part of the Brillouin zone were needed for accurately reconstructing the Fock matrix during the self-consistent iterative procedure. Details of density functional theory (DFT) method embodied in CRYSTAL98 are given elsewhere [22].

The method CASTEP[23] employs DFT and is based on the generalised-gradient approximation (GGA). Perdew-Burke-Ernzerhof (PBE) is used as exchange-correlation functional [24]. Non-local ultra-soft pseudopotentials generated by the method of Vanderbilt [25] are used to describe electron-ion interactions. The pseudo atomic calculations are performed for Li ($1s^2$ $2s^1$) and N ($2s^2$ $2p^3$). The valence electron wavefunctions are expanded in a plane wave basis set with a kinetic energy cut-off of 300 eV. This converges the total energy of the system to better than 0.001eV/atom. Brillouin zone integrations are performed on a Monkhorst-Pack grid that is taken large enough to reach a similar level of convergence in total energy as the wavefunction cut-off.

3. Calculations, Results and Discussions

3.1. *Structural and elastic properties of α- and β-phases*

The total energy E of Li_3N has been calculated at different primitive cell volume. The energy was minimized as a function of the c/a ratio for selected values of volume. The zero pressure bulk modulus B_0 and its pressure derivative B_0' (=dB/dP) are determined by fitting the $E \sim V$ curve (not shown) by the Murnaghan equation-of-state [26]. The optimized structural parameters, bulk modulus and its pressure derivative are given in Table 1, along with other theoretical results and available experimental measurements. It is seen that the calculated lattice parameters are better in the present study and agree well with experiments [8].

Table 1. Lattice constants, bulk modulus and pressure derivative of bulk modulus for Li_3N at ambient conditions.

Phase	Method	a (Å)	c(Å)	B_0 (GPa)	B'_0	Ref.
	HF-CRYSTAL	3.61	3.84	-	-	[17]
	HF-CRYSTAL98	3.6413	3.8751	63.9	4*	This
α–phase	DFT-CRYSTAL98	3.6289	3.823	72.6	4*	This
	CASTEP	3.6643	3.9315	-	-	This
	Q-ESPRESSO	3.534	3.772	58.9	3.8	[13]
	LDA-Ultrasoft	3.508	3.745	61.0	3.7	[11]
	Expt.	3.648	3.875	-	-	[8]
	DFT-CRYSTAL98	3.558	6.250	98	4.04	This
β-phase	CASTEP	3.5789	6.3602	-	-	This
	Q-ESPRESSO	3.445	6.148	74.5	3.42	[13]
	LDA-Ultrasoft	3.418	6.100	78.2	3.77	[11]
	Expt.	3.552	6.31	-	-	[8]

* Kept fixed during fitting.

The normalized lattice constants a/a_0 and c/c_0 (where a_0 and c_0 are the zero-pressure equilibrium lattice constants) as a function of pressure up to 35 GPa are shown in Fig. 1.

By fitting these data to third order polynomials of pressure, we obtain the following relationships at $T = 0$:

$$a/a_0 = 1.0016 - 5.7\times10^{-3}P + 10^{-4}P^2 - 1.41\times10^{-6}P^3$$
$$c/c_0 = 1.0017 - 5.2\times10^{-3}P + 10^{-4}P^2 - 1.40\times10^{-6}P^3$$

It is obvious that, as the pressure increases, the compression along the c-axis is roughly of the same order as in the a-axis in the basal plane. Fig. 2 shows the normalized volume V_n ($=V/V_o$, V_o= equilibrium volume) of β-phase (D^4_{6h} structure) as a function of pressure up to P = 35 GPa. The equation of state EOS of the $D_{6h}{}^4$ phase has been measured up to 35 GPa [11]. The experimental P-V_n data points[8] are plotted in the same figure which shows nice agreement with our *ab initio* calculation.

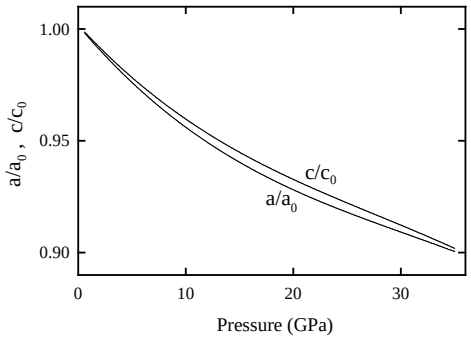

Fig. 1. Lattice parameters a/a_o and c/c_o as a function of pressure.

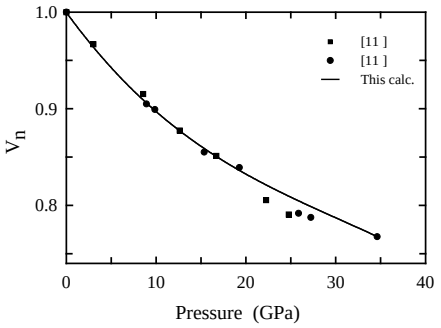

Fig. 2. The calculated EOS of Li_3N. Solid squares and solid circles represent experiment [11].

3.2. *Single crystal elastic constants of α- and β-phases*

The finite strain method is the most commonly used method for computation of stiffness coefficients and this one is used in the present work. We shall consider only small lattice distortions in order to remain within the elastic limit of the crystal. The internal energy of a crystal under strain δ can be expanded in powers of the strain tensor with respect to the initial internal energy of the unstrained crystal. The energy of a strained system [27, 28] can be expressed in terms of the elastic constants C_{ij} as:

$$E(V,\delta) = E(V_0,0) + V_0\left[\sum_i \tau_i\xi_i\delta_i + \tfrac{1}{2}\sum_{ij} C_{ij}\delta_i\xi_i\delta_j\xi_i\right] \quad (1)$$

where $E(V_0,0)$ is the energy of the unstrained system with volume V_0. τ_i is an element in the stress tensor, ξ_i is a factor to take care of Voigt index.

There are five independent components of the elasticity tensor for the hexagonal Li_3N, instead of three as in the cubic case. The energy corresponding to five distinct lattice deformations can now be obtained. The second order term in the expression of the strain energy as a function of deformation parameter δ is related to a particularly simple

condition of different elastic constants as shown Table 2. Stresses used to calculate the elastic constants at zero pressure are as listed in the table.

Table 2. Stresses for the calculation of elastic constants at P=0.

Type of distortion	Energy for the distorted crystal	$\frac{1}{V_0}\frac{\partial^2 E}{\partial \delta^2}$
Changes size of basal plane, z constant	$E(V_0,0)+V_0[(\tau_1 + \tau_2)\delta + (C_{11} + C_{12})\delta^2]$	$2(C_{11} + C_{12})$
z-axis constant, x increases, y decreases by equal amount	$E(V_0,0)+V_0[(\tau_1 - \tau_2)\delta + (C_{11} - C_{12})\delta^2]$	$2(C_{11} - C_{12})$
Stretches z-axis, other axes unchanged (maintains symmetry)	$E(V_0,0)+V_0[(\tau_3\delta + \frac{1}{2} C_{33}\delta^2]$	C_{33}
Changes V, preserves symmetry	$E(V_o,0)+V_0[(\tau_1 + \tau_2+ \tau_3)\delta + \frac{1}{2}(2C_{11}+2C_{12}+4C_{13}+C_{33})\delta^2]$	$2C_{11}+2C_{12}+4C_{13}+C_{33}$
V-conserving triclinic distortion	$E(V_0,0)+V_0[(\tau_4\delta + 2C_{44}\delta^2]$	$4C_{44}$

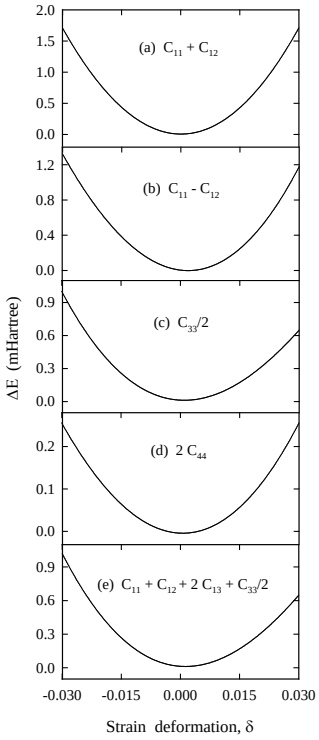

Fig. 3. Strain energy of α-Li_3N as a function of δ, for the five different strains.

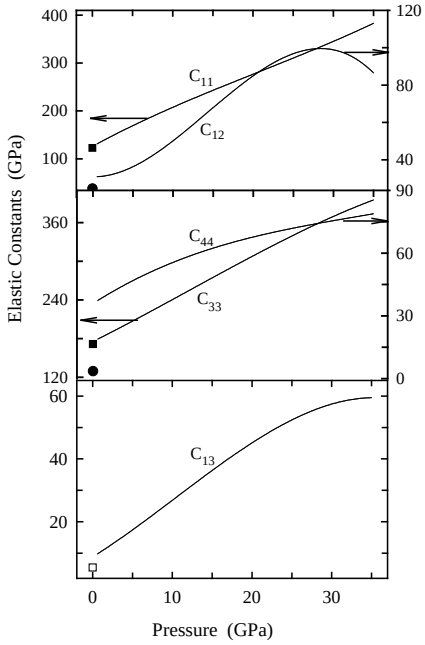

Fig. 4. Calculated elastic constants of β-Li_3N as a function of pressure. The zero pressure data points are only for the α-phase.

The energy was calculated using the appropriate expression corresponding for each of the five distinct lattice distortions. The results of the dependence of [*E (V, δ)-E (V$_0$, δ)*] on δ for α-Li_3N using DFT-CRYSTAL98 calculations are shown in Fig. 3. In the second approach using CASTEP, the ground state structure is strained according to symmetry-dependent strain patterns with varying amplitudes and a subsequent computing of the stress tensor after a re-optimization of the internal structure parameters, i.e. after a geometry optimization with fixed cell parameters. The elastic stiffness coefficients are then the proportionality coefficients relating the applied strain to the computed stress. The calculation of the elastic constants involves second derivatives of the total energy with respect to lattice distortion. This implies a lowering of the crystal symmetry and because the strain energy is very small, the relative error will certainly be larger than for isotropic properties such as equilibrium volume which needs only the first derivatives of the total energy. From the precision of our total energy results and other calculations we consider the present approach is adequately precise which is necessary for the calculation of the elastic constants.

Table 3. Elastic constants C_{ij} (in GPa) of Li_3N in α- and β-phases at ambient pressure.

Phase	C_{11}	C_{12}	C_{13}	C_{33}	C_{44}	Method
α-phase	165.7	22.7	8.3	180.0	18.1	HF -CRYSTAL98
	162.3	26.3	4.5	183.5	14.4	DFT-CRYSTAL98
	122.8	24.6	5.4	129.5	16.6	CASTEP
	114	38	-	118	17	Derived*
β-phase	215	25.9	7.5	219.8	40.1	DFT-CRYSTAL98
	131.8	28.8	8.7	180.4	37.1	CASTEP

*Derived from measured phonon dispersion curves [14].

The calculated results of C_{ij} for α- and β–Li_3N at ambient conditions using different computational methods are shown in Table 3 along with those determined from the slopes of the acoustic branches in the long wavelength region of the measured phonon dispersion curves [14]. A comparison of the calculations with the derived quantities determined as above, the CASTEP-calculated elastic constants at ambient conditions seem to yield better results.

The elastic constants C_{ij} of β–Li_3N are also calculated as a function of pressure using CASTEP and the results are shown in Fig. 4. The zero-pressure elastic constants are also plotted in the same figure. The figure shows that all the elastic constants of β–Li_3N increase with pressure but by different rates. C_{12} steadily increases and then goes down after ~30 GPa. The same trend is also observed in the case of C_{13}. C_{44} first increases and then the rate of its increase decreases. It may be mentioned here that a new γ–phase appears at ~ 28-40 GPa [12].

3.3. *Debye temperature and elastic properties of polycrystalline aggregate of α- and β-phases*

The Debye temperature Θ_D is an important quantity and closely related to many physical properties of solids, such as specific heat and melting temperature. For temperature less than Θ_D quantum mechanical effects are very important in understanding the thermodynamic properties. The Debye temperature is also used to estimate the electron-phonon coupling constant λ, which is proportional to the mean sound velocity v_m [29].

$$\Theta_D = \frac{h}{k_B}\sqrt[3]{\frac{3n}{4\pi\Omega}}\ v_{\mathbf{m}}, \quad \frac{3}{v_m^3} = \frac{1}{v_l^3} + \frac{2}{v_s^3}, \tag{2}$$

where h is Planck's constant, k_B is Boltzmann's constant, n is the number of atoms per formula unit and Ω (= $M/N_A\rho$, M = molecular weight, N_A = Avogadro's number, ρ = density) is the mean atomic volume. v_l and v_s are the longitudinal and transverse sound velocities.

The theoretical polycrystalline elastic moduli for Li_3N may be calculated from the set of five independent elastic constants. Hill [30] proved that the Voigt and Reuss equations represent upper and lower limits of the true polycrystalline constants. He showed that the polycrystalline moduli are the arithmetic mean values of the Voigt and Reuss moduli, and are thus given by $B_H \equiv B = ½(B_R + B_V)$ and $G_H \equiv G = ½(G_R + G_V)$. The Reuss and Voigt bulk moduli for hexagonal Li_3N are given by (see [31]):

$$B_R = \frac{C_{33}(C_{11}+C_{12}) - 2C_{13}^2}{C_{11}+C_{12}-4C_{13}+2C_{33}} \tag{3}$$

$$B_V = \tfrac{2}{9}(C_{11}+C_{12}+2C_{13}+\tfrac{1}{2}C_{33}) \tag{4}$$

Similarly the shear moduli are given by

$$G_R = \frac{5}{2}\frac{[(C_{11}+C_{12})C_{33}-2C_{13}^2]^2}{3B_VC_{44}C_{66}+[(C_{11}+C_{12})C_{33}-2C_{13}^2]^2(C_{44}+C_{66})} \tag{5}$$

$$G_V = \tfrac{1}{30}(C_{11}+C_{12}+2C_{33}-4C_{13}+12C_{44}+12C_{66}) \tag{6}$$

where $C_{66} = \tfrac{1}{2}(C_{11}-C_{12})$ ` (7)

The probable values of the average shear and longitudinal sound velocities can be calculated from Hill's equations as follows:

$$v_s = (G_H/\rho)^{1/2}, \quad v_l = [(B_H + 4/3G_H)/\rho]^{1/2} \tag{8}$$

The polycrystalline Young's modulus (E) and the Poisson's ratio (υ) are then calculated using the relationships (see [31]): $E = 9BG/(3B + G)$ and $\upsilon = (3B - 2G)/(6B + 2G)$.

Fig. 5 shows the variation of sound velocities of β-Li_3N as a function of pressure. Both the longitudinal and transverse sound velocities increase as the pressure is increased. The

aggregate bulk, shear and Young's moduli (*B, G, E*) and the Poisson's ratio υ are shown in Fig. 6 as a function of pressure. In both the figures zero pressure values α-Li_3N have also been plotted. It is seen that both the bulk and shear moduli increase as pressure is increased, but they do so in a different rate, particularly at higher pressure. We see that the Young's modulus and the Poisson's ratio also increase with the increase of pressure but certainly there are small behavioural changes for P ~30 GPa. It is to be noted here that a new phase has been predicted at P = 27.6 GPa [32]. But more recently Lazicki *et al.* [12] has shown that β-phase indeed transforms to γ-Li_3N, but in the pressure range of 36-45 GPa.

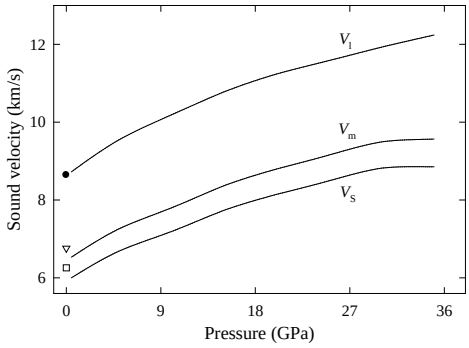

Fig. 5. Longitudinal and transverse sound velocities of Li_3N as a function of pressure. The zero pressure data points (v_l - solid circle, v_m - inverted triangle, v_s - open square) are for the α-phase.

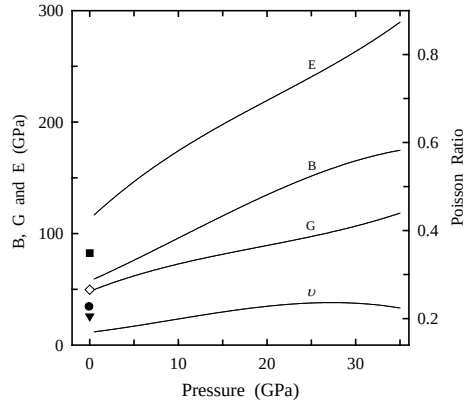

Fig. 6. Bulk, shear, Young's moduli and Poisson's ratio of Li_3N as a function of pressure. All the zero pressure data points (*E*- solid square, *B* - diamond, *G* - solid circle, ν - inverted triangle) are for the α-phase.

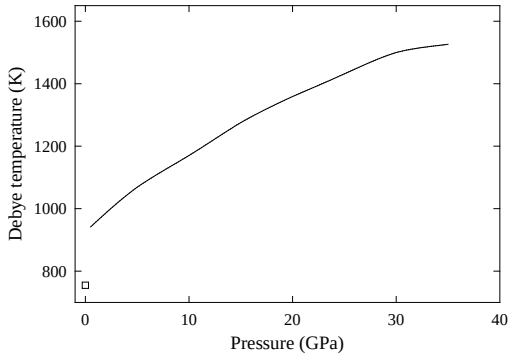

Fig. 7. The Debye temperature Θ_D as a function of pressure. The zero pressure point (solid square) is for α-Li_3N.

Using the single-crystal elastic constants of Li_3N, we obtain Debye temperatures Θ_D for α-Li_3N at ambient conditions and for β-Li_3N as a function of pressure (Fig. 7). The density ρ has been assumed to be pressure dependent while calculating pressure dependent quantities mentioned above in Eqs. (2-8)**.** The value of Θ_D= 755 K for α-Li_3N at P = 0 may be compared to 1016K for MgB_2 [33] and 743K for TiB_2 [34]. It is thus

found that the value is closer to that of TiB_2 than to MgB_2.Further Θ_D increases as pressure increases.

We notice that the average values for anisotropy factor A $(=C_{11}/C_{33})$ at ambient condition are 0.93 and 0.85 for α-Li_3N and β-Li_3N, respectively. Although the anisotropy factor is by no means sufficient to confirm the anisotropy of the system, our results, however, do indicate a very small anisotropy.

4. Conclusions

We have investigated the equilibrium structure, elastic properties including five independent elastic constants and Debye temperature of Li_3N using three different computational methods. Both the hexagonal D^4_{6h} ($P6_3/mmc$) and the hexagonal D^1_{6h} ($P6/mmm$) structures at ambient and higher pressures are considered. The equilibrium lattice parameters obtained are better than other theoretical results and in very good agreement with the available experimental data. No theoretical or experimental data for single crystal elastic constants, the aggregate elastic moduli (B, G, E), the Poisson's ratio (ν), and the Debye temperature Θ_D are yet available for comparison. A comparison of the calculated single crystal elastic constants with the derived quantities determined from the slopes of the acoustic branches in the long wavelength region of the measured phonon dispersion curves show that the CASTEP-calculated elastic constants at ambient conditions seem to reproduce better results. It is found that the Debye temperature of α-Li_3N is closer to that of TiB_2 than to MgB_2.

References

1. A. Rabenau, *in* Festkorperprobleme (Advances in Solid State Physics) edited by J. Treusch (Vieweg, Braunschweig, 1978), vol. 18, pp. 77-108.
2. P. Chen, Z. Ziong, J. Luo, J. Lin, and K. Lee Tan, Nature (London) **420**, 302 (2002). doi:10.1038/nature01210
3. T. Ichikawa, S. Isobe, N. Hanada, and H. Fujii, J. Alloys Compd. **365**, 271 (2004). doi:10.1016/S0925-8388(03)00637-6
4. Y. H. Hu, E. Ruckenstein, Ind. Eng. Chem. Res. **44**, 1510 (2005). doi:10.1021/ie0492799
5. Y. Nakamori, G. Kitahara, K. Miwa, S. Towata, and S. Orimo, Appl. Phys. A: Mater. Sci. Process. **80**, 1 (2005). doi:10.1007/s00339-004-3002-6
6. Y. Xie, Y. Qian, W. Wang, S. Zhang, and Y. Zhang, Science **272**, 1926 (1996). doi:10.1126/science.272.5270.1926
7. E. Zintl and G. Brauer, Z. Elektrochem. Angew. Phys. Chem. **41**, 102 (1935).
8. H. J. Beister, Sabine Haag et al., Angew. Chem, Int. Ed. Engl. **27**, 1101 (1988). doi:10.1002/anie.198811011
9. M. Mali, J. Roos, and D. Brinkmann, Phys. Rev. B **36**, 3888 (1987). doi:10.1103/PhysRevB.36.3888
10. S. Mitrohina, K. Burdina, and K. Semeneko, Moscow Univ. Chem. Bull. **45**, 89 (1990).
11. A. C. Ho, M. K. Granger, A. L. Ruoff, P. E. Van Camp, and V. E. Van Doren, Phys. Rev. B **59**, 6083 (1999). doi:10.1103/PhysRevB.59.6083
12. A. Lazicki, B. Maddox, W. J. Evans, C. S. Yoo, A. K. McMahan, W.E. Pickett, R.T. Scalettar, M.Y. Hu, and P. Chow, Phys. Rev. Lett. **95**, 165503 (2005). doi:10.1103/PhysRevLett.95.165503
13. Y. Yan, J. Y. Zhang, T. Cui, Y. Li, Y. M. Ma, J. Gong, Z. G. Zong, and G. T. Zou, Eur. Phys. J. B **61**, 397 (2008). doi:10.1140/epjb/e2008-00107-0

14. W. Kress, H. Grimm, W. Press, and J. Lefebvre, Phys. Rev. B **22**, 4620 (1980). doi:10.1103/PhysRevB.22.4620
15. G. Kerker, Phys. Rev. B **23**, 6312 (1981). doi:10.1103/PhysRevB.23.6312
16. H. R. Chandrasekhar, G. Bhattacharya, R. Migoni, and H. Blitz, Phy. Rev. B **17**, 884 (1978). doi:10.1103/PhysRevB.17.884
17. R. Dovesi, C. Pisani, F. Ricca, C. Roetti, and V. R. Saunders, Phys. Rev. B **30**, 972 (1984). doi:10.1103/PhysRevB.30.972
18. P. Blaha, J. Redinger, and K. Schwarz, Z. Phys. B **57**, 273 (1984).
19. J. Sarnthein, K. Schwarz, and P. E. Blöch, Phys. Rev. B **53**, 9084 (1996). doi:10.1103/PhysRevB.53.9084
20. A. Huq, J. W. Richardson, E. R. Maxey, D. Chandra, and Wen-Ming Chien, J. Alloys. Compd. **436**, 256 (2007). doi:10.1016/j.jallcom.2006.07.021
21. V. R. Saunders, R. Dovesi, C. Roetti, M. Causa, N. M. Harrison, R. Orlando, and C. M. Zicovich-Wilson, CRYSTAL98 User's Manual, University of Torino, Torino, 1998.
22. M. A. Hossain, M.Sc Thesis, Rajshahi University (2005).
23. S. J. Clark, M. D. Segall, C. J. Pickard, P. J. Hasnip, M. J. Probert, K. Refson, and M. C. Payne, Zeitschrift fuer Kristallographie **220** (5-6), 567 (2005). doi:10.1524/zkri.220.5.567.65075
24. J. P. Perdew, K. Burke, and M. Ernzerhof, Phys. Rev. Lett, **77**, 3865 (1996). doi:10.1103/PhysRevLett.77.3865
25. D. Vanderbilt, Phys. Rev. B **41**, 7892 (1990). doi:10.1103/PhysRevB.41.7892
26. F. D. Murnaghan, Proc. Natl. Acad Sci. USA **30**, 244 (1944). doi:10.1073/pnas.30.9.244
27. L. Fast, J. M. Wills, B. Johansson, O. Eriksson, Phys. Rev. B **51**, 17431 (1995). doi:10.1103/PhysRevB.51.17431
28. J. F. Nye, Physical Properties of Crystals (Oxford University Press, London, 1967) chapter 8.
29. O. L. Anderson, J. Phys. Chem. Solids **24**, 909 (1963). doi:10.1016/0022-3697(63)90067-2
30. R. Hill, Proc. R. Soc. London Ser. A **65**, 350 (1952).
31. K. B. Panda, K.S. Ravi Chandran, Comput. Materials Science **35**, 134 (2006). doi:10.1016/j.commatsci.2005.03.012
32. J. C. Schön, M. A. C. Wevers, M. Jansen, J. Mater. Chem. **11**, 69 (2001). doi:10.1039/b002956o
33. S. L. Bud'ko, G. Lapertot, C. Petrovic, C. E. Cunningham, N. Anderso, P. C. Canfield, Phys. Rev. Lett. **86**, 1877 (2001). doi:10.1103/PhysRevLett.86.1877
34. P. S. Spoor, J. D. Maynard, M. J. Pan, D.J. Green, J. R. Hellmann, T. Tanaka, Appl. Phys. Lett. **70**, 1959 (1997). doi:10.1063/1.118791

Note added (25 May 2012): Corrections to Fig. 5 and Fig. 7 made.